ACS APPLIED MATERIALS & INTERFACES

Research Article

www.acsami.org

Design and Fabrication of Superamphiphobic Paper Surfaces

Lester Li,[†,‡] Victor Breedveld,[†] and Dennis W. Hess*[,†]

[†]School of Chemical and Biomolecular Engineering, Georgia Institute of Technology, 311 Ferst Drive, Atlanta Georgia 30332, United States

[‡]Institute of Paper Science and Technology, Georgia Institute of Technology, 500 10th Street Northwest, Atlanta, Georgia 30318, United States

ABSTRACT: Cellulose-based paper remains a vital component of modern day society; however, its use is severely limited in certain applications because of hydrophilic and oleophilic properties. In this manuscript we present a novel method to create superamphiphobic paper by combining the control of fiber size and structure with plasma etching and fluoropolymer deposition. The heterogeneous nature of the paper structure is drastically different from that of artificially created superamphiphobic surfaces. By refining the wood fibers, smaller diameter fibers (fibrils) are created to support fluid droplets. After oxygen plasma etching and deposition of a fluoropolymer film, paper samples are able to support motor oil contact angles of 149 ± 3°, although these structures readily absorb *n*-hexadecane. Exchange of water in the pulp solution with sec-butanol provides additional control over fiber spacing to create superamphiphobic substrates with contact angles >150° for water, ethylene glycol, motor oil, and *n*-hexadecane.

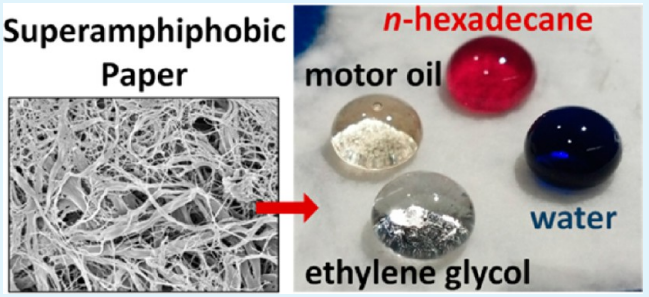

KEYWORDS: *superamphiphobic, superoleophobic, superhydrophobic, paper, cellulose, plasma*

INTRODUCTION

Because of their fascinating chemistry and physics, along with numerous potential applications, superhydrophobic surfaces have been investigated in great detail over the past several decades.[1−7] Defined as having a static water contact angle greater than 150°, such surfaces have been developed on a plethora of inorganic and organic surfaces. However, the majority of superhydrophobic surfaces are unable to support elevated contact angles for reduced surface tension fluids such as oils; as a result, highly oil repellent (superoleophobic) surfaces with static oil contact angles greater than 150° are generally difficult to achieve unless carefully engineered surface structures are used.[8−10] Our investigation focuses on the development of paper substrates that simultaneously exhibit superhydrophobic and superoleophobic properties; such universally nonwetting substrates are often referred to as superamphiphobic.[11] The critical parameters for these superamphiphobic surfaces are a specific combination of low surface energy and reentrant surface structures.[8] Such surfaces have been constructed on rigid inorganic substrates through nanoscale fabrication techniques, commonly resulting in delicate, brittle structures.[9,12−14] In contrast, paper is a biodegradable, renewable, inexpensive material that is produced worldwide on an industrial scale. The aforementioned properties and broad availability of paper have led to expansion of its use in novel, technologically advanced fields, such as paper-based microfluidics in the biomedical industry.[15,16] However, the naturally occurring hydrophilic and oleophilic properties of cellulose-based paper continue to greatly restrict the scope of its applications. To inhibit water absorption, our group[17,18] and others[19,20] have developed surface modifications of common paper substrates to attain superhydrophobic properties. Despite the advances made through these studies, superoleophobic fiber based paper has yet to be reported. Cellulose-based superoleophobic surfaces have been reported in the form of aerogels[21,22] and cellulose-coated structured silicon,[23] but these substrates lack the availability and manufacturability of traditional paper. Spray coating of paper has also been utilized to create superoleophobic surfaces, but this approach relies entirely on the coating properties rather than exploiting the inherent properties of the fiber network.[24] Jin et al. have demonstrated amphiphobicity on filter paper using liquid treatments to generate the necessary roughness and hydrophobic surface chemistry; however, fiber structure requirements were not described nor discussed, and the study was limited to filter paper, which is a specialty paper in the sense that it is designed to withstand prolonged exposure to liquids.[25] Oil-repellent paper products that can be manufactured via scalable processes are of great interest for the paper industry, with applications in fluid and materials packaging. Perhaps even more important is the opportunity to expand the use of paper products into other fields such as the biomedical industry where disposable, bacteria-resistant surfaces and test strips can be envisioned.[25]

Past studies have demonstrated that attainment of superoleophobicity relies heavily on distinct roughness geo-

Received: April 19, 2013
Accepted: May 6, 2013
Published: May 6, 2013

metries.[8,26−29] Specifically, the contact angles of low surface tension fluids are enhanced by surface structures with reentrant angles. To simplify the manufacturing process for creating reentrant structures and expand the scope of available substrate materials, researchers have turned their attention to fiber- and wire-based substrates with well-defined, uniform, ordered repeat structures. The salient aspect here is that the bottom half of a cylindrical fiber offers reentrant angles or overhang constructs that are similar to lithographically created structures. Exploiting this concept, superoleophobic surfaces have been developed on highly ordered, uniform mesh screens and woven fabrics.[8,30−35] These studies have highlighted the fact that the critical physical parameters of superoleophobic substrates are the dimensions and spacing of the structures.

The most commonly cited models to describe wetting behavior on roughened surfaces are the Wenzel[36] and Cassie−Baxter[37] models. In the Wenzel model, fluid is assumed to be in complete contact with the enhanced surface area generated by roughness, whereas in the Cassie−Baxter state the droplet is supported by air pockets trapped between the surface structures, thus reducing the liquid−solid contact area. To attain high oil contact angles on a surface, the fluid must maintain a Cassie−Baxter wetting state.[8,9,14] To model fiber-based substrates, modifications to the Cassie−Baxter equation have been made to yield

$$\cos\theta^* = \frac{D(\pi - \theta^e)}{L}\cos\theta^e + \frac{D}{L}\sin\theta^e - 1 \quad (1)$$

where the apparent contact angle (θ^*) is a function of the center-to-center distance between two fibers (L), the fiber diameter (D), and equilibrium contact angle (θ^e).[31,38,39] The size and spacing of surface structures can easily be varied when produced lithographically, whereas for fiber-based mesh screens and woven fabrics, L and D are established by the manufacturing process, fiber size, and weave. However, many surfaces of significant scientific and technological interest do not have such well-defined structures.

Herein we present an approach to the design and fabrication of superamphiphobic paper substrates that exploits the physical properties of the heterogeneous fiber web. This novel achievement is accomplished by systematically altering the average fiber size and interfiber spacing through a combination of techniques: fiber refining prior to paper formation, solvent exchange during paper formation, and plasma processing post-treatment of the paper. Beyond the inherent hydrophilicity and oleophilicity of cellulose fibers, the greatest challenge in fabricating superamphiphobic paper remains the creation of fibrous structures with the correct length scales. At the micrometer scale, paper is composed of cellulose fibers that are heterogeneously spaced and randomly oriented. Highly oleophobic substrates made from randomly oriented fibers have proven nontrivial to produce.[8,25,26] Unlike previous reports, which utilize uniform polymeric fibers, nature constrains our options by supplying cellulosic fibers for paper production only in specific size ranges. To compound the difficulties, processed fibers are often not circular in shape, but ellipsoidal (see inset in Figure 1a). These factors combine to define paper as a complex material with randomly oriented and sized fibers that that display a surface structure that contrasts greatly with the carefully crafted, highly ordered superoleophobic surface geometries that have been reported to date.

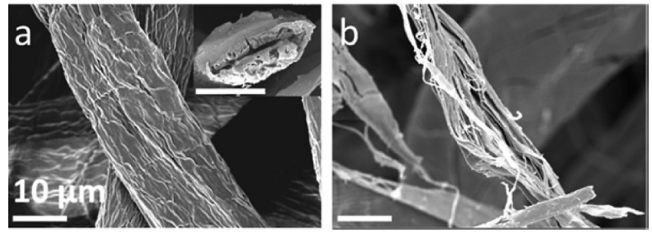

Figure 1. SEM images of (a) unrefined and (b) refined fibers, highlighting the effects of refining on the fiber structure. Inset in a depicts the cross-section of an unrefined fiber. Scale bars represent 10 μm.

EXPERIMENTAL METHODS

Pulp Refining. For this manuscript, southern hardwood Kraft fibers (Alabama River Pulp Co.) were used. The fibers were refined according to TAPPI standardized method T 248 sp-08,[40] whereby dry fiber sheets were soaked in deionized water overnight and then loaded in a PFI (Pulp and Fiber Research Institute) refiner (Test Machines Inc.) and exposed to different levels of refining as defined by the number of revolutions.

Handsheet Formation. Handsheets were formed using two different methods. When processed with water, handsheets were formed following TAPPI standardized method T 205 sp-02, whereby the refined pulp is lowered in consistency and then drained under gravity onto a mesh screen. The handsheet is subsequently pressed and dried overnight on a stainless steel plate. For handsheets made using *sec*-butanol (Alfa Aesar, anhydrous, 99%), the refined pulp is first drained through a 75 μm pore mesh screen. The water filtrate is discarded and *sec*-butanol (100 mL) is added to the drained pulp. The pulp is then remixed for 2 min and again drained through a 75 μm screen. After the *sec*-butanol/water mixture has drained from the pulp, the sheet is pressed and then dried overnight on a stainless steel plate.

Plasma Etching and Fluoropolymer Deposition. Paper samples were etched and subsequently exposed to fluorocarbon film deposition in a parallel plate (13.56 MHz) vacuum plasma reactor. Both steps were conducted at 110 °C using a power of 120 W. To etch the paper, oxygen was introduced to the reactor at 75 standard cubic centimeters per minute (SCCM), and allowed to reach an equilibrium pressure of 5.0×10^{-1} Torr. The fluoropolymer coating was deposited using a plasma composed of 40 SCCM Ar and 20 SCCM pentafluoroethane (Praxair) at an operating pressure of 1.0 Torr. While etch times were varied, the deposition step was constant at 2 min, for all studies described below, yielding a coating thickness of ∼400 nm. More detailed descriptions regarding the procedure and reactor configuration can be found in previous publications.[17]

Contact Angle Measurements. All static contact angle measurements were performed by placing a 4 μL droplet of the selected fluid (DI water, ethylene glycol (BDH, reagent grade), motor oil (SAE 10W-30, MotoTech) or *n*-hexadecane (Sigma-Aldrich Co., 99%)) onto the paper surface and then recording an image using a Lumenera LU135c camera equipped with a Leica A6 APO zoom lens. Contact angle analysis was performed using the DropSnake program in ImageJ image analysis software (NIH). This method was used in lieu of a standard goniometer's fitting program largely because of poor modeling of droplets of low surface tension fluids that, even at the relatively small volumes analyzed in this study, become aspherical at high contact angles.

SEM Imaging. All samples subjected to scanning electron microscopy (SEM) imaging were sputter coated with Ag/Pd to mitigate charging effects. Images were taken with a Zeiss Ultra60 FE-SEM at an electron energy of 5.0 keV.

Profilometer Measurements. Measurements were conducted using a Wyko NT2000 Optical Profilometer. R_a values were analyzed using the Vison32 sofware (Veeco Instruments Inc.), calculated per the ANSI B46.1 standard. Surface coverage analysis was conducted by processing the raw profilometer height profiles in MATLAB (The

Mathworks, Inc.) by applying filtering and thresholding procedures on the height profile data to identify the top fiber layer.

RESULTS AND DISCUSSION

Fiber Refining. To control the fiber spacing (L) and diameter (D) parameters of paper, pulp refining was applied. Industrially, refining is a commonly practiced technique used to increase the uniformity and strength of paper products;[41] fibrous pulp is ground between metal gears, thereby shearing or fibrillating the individual fibers. Figures 1a and b show scanning electron micrograph (SEM) images of an unrefined and refined hardwood fiber, respectively. The refined fiber shown in Figure 1b was processed using the special solvent exchange process discussed below to illustrate the effect of refining on an individual fiber. An increase in refining intensity ultimately separates fibers into their elementary components, so-called fibrils (see Figure 1b), much like a braided rope can be deconstructed into many smaller diameter cords. In order to ensure that our studies solely investigate the physical effects of the fibers, and not the properties of chemical modifiers and fillers present in commercial paper products, we create our own paper substrates without additives. Our paper substrates, composed of only natural wood fibers, are termed handsheets in this manuscript. Figures 2a–f present SEM images and

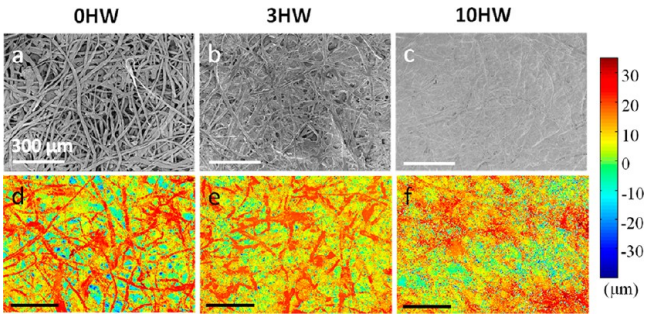

Figure 2. SEM images of 0, 3, and 10HW handsheets are shown in (a–c), respectively, demonstrating that increased refining smooths the handsheet surface. Complementary profilometer images are presented in (d–f). All scale bars correspond to 300 μm.

roughness profiles measured with optical profilometry for handsheets made from hardwood pulp subjected to varying levels of refining. In the following discussion, we will classify the substrates by designations that contain the number of revolutions (in thousands) experienced in the PFI refiner and wood type (i.e., handsheets made from hardwood pulp exposed to 3000 revolutions are denoted "3HW"). SEM and profilometer data indicate that increased refining intensity leads to less porous handsheets, in which individual fibers become difficult to identify. At high refining levels, hydrogen bonding between fibrils (seen in Figure 1b) creates agglomerates that fill interstitial pore spaces in the fibrous network, leading to a smoother appearance of the handsheet. Refining thus offers control over the size distribution of the fibers, characterized by parameter L in eq 1.

The next challenge to achieving superamphiphobic paper surfaces is to control the inherent wetting properties of the fibers. In previous work, our group has used plasma etching to selectively remove the amorphous phase of cellulose, leaving behind crystalline phase protrusions from the fiber surface. This process creates nanoscale roughness on the surface of individual fibers, and micrometer-scale roughness after extended etch times.[17] When followed by plasma deposition of a fluorocarbon film from a pentafluoroethane precursor, the two-step process renders the surface superhydrophobic.[17] In this study, handsheets made from 0, 1, 3, 5, and 10HW pulp were etched for different durations, followed by deposition of a 400 nm fluoropolymer film. After 15 min of etching (and fluoropolymer deposition), all handsheets exhibit superhydrophobic properties (see Figure 3a), but the wetting behavior for oils shows much greater diversity and dependence on etch time. Static contact angles of motor (γ_{lv} = 32.2 mN m^{-1})[42] and n-hexadecane (γ_{lv} = 27.5 mN m^{-1}) on handsheets with various levels of refining are presented in panels b and c in Figure 3 as a function of etch time. Although these two fluids have similar surface tensions, their contact angles are drastically different for the same processing conditions. Utilizing n-hexadecane as a test fluid, short etch times yield a large increase in contact angles, with a 15 min etch time changing 0, 1, 3, and 5HW handsheets from completely absorbing to slightly oleophobic. We believe that this increase in contact angle is due to the formation of a dual-scale, hierarchical surface when nanoscale roughness formed by the plasma etching is combined with the micrometer-scale roughness of the fiber network. Figure 4 shows SEM images of a 0HW handsheet etched for various times, with and without a fluoropolymer deposition. Clearly, as etch time is increased to 30 min, nanoscale roughness is formed on individual fibers, and after 90 min of etching, the fibers have been etched to a skeletonized version of the original fiber. The reduction of n-hexadecane contact angles to a zero value at the longer etch times is due to fiber destruction, causing the fibrils to collapse under the weight of a droplet; this results in a wetting transition from the Cassie–Baxter to the Wenzel state. In comparison with handsheets formulated from pulp subjected to other refining levels, 10HW handsheets behave quite differently.

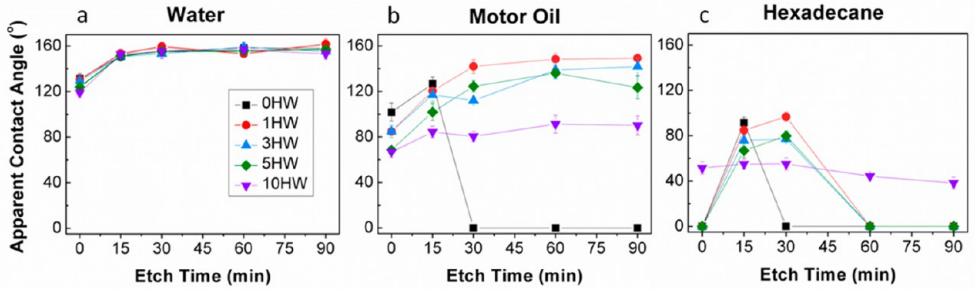

Figure 3. Apparent contact angle measurements of (a) water, (b) motor oil, and (c) n-hexadecane for handsheets made from pulp at various refining levels as a function of oxygen plasma etch time.

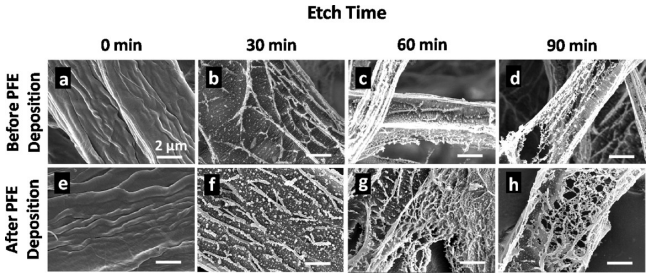

Figure 4. SEM images of fibers that have been etched for (a, e) 0, (b, f) 30, (c, g) 60, and (d, h) 90 min, before and after deposition of 400 nm of PFE.

Figure 3a–c demonstrates that 10HW handsheets are relatively unaffected by plasma etching, neither increasing nor decreasing the contact angles significantly for either fluid. This atypical behavior results from the large number of fibrils that agglomerate to form a dense, continuous surface for the highly refined sample (see Figure 2c). In fact, the measured contact angles are similar to the equilibrium contact angles for *n*-hexadecane ($\theta^{e}_{n\text{-hexadecane}} = 42 \pm 2°$) on a flat silicon wafer after plasma deposition of the same fluoropolymer. Thus, although increased refining yields a greater number of small diameter fibrils, strong interfiber hydrogen bonding binds them together, resulting in a smooth, nonporous surface. To effectively utilize the refined fibrils to stabilize the Cassie–Baxter state, clustering must be inhibited.

Solvent Exchange Processing. To enhance the separation of fibers and fibrils (parameter *D* in eq 1), we employ a solvent exchange method, whereby the fibrous pulp is drained of water and then added to *sec*-butanol; the pulp is then drained of the *sec*-butanol and dried without subsequent exposure to water. Organic solvents have been demonstrated to prevent hydrogen bonding between cellulosic fibers.[43,44] In our case, *sec*-butanol is employed to prevent the fibrils created during the refining process from binding together, thereby significantly increasing the sheet porosity. However, by inhibiting fiber–fiber hydrogen bonding, a decrease in the strength of the handsheet is also observed; this effect will be quantified in subsequent studies. Comparison of Figures 5a and 2a underlines the dramatic difference between the structure of handsheets made from 10HW pulp when processed with *sec*-butanol and water, respectively. A higher-magnification image of a *sec*-butanol processed handsheet (Figure 5b) clearly reveals the separation of micrometer and submicrometer scale fibers. Figure 6 presents the variation of contact angle with etch time on these handsheets for four liquids: water, ethylene glycol (γ_{lv} = 48.4 mN m^{-1}), motor oil and *n*-hexadecane. Without etching,

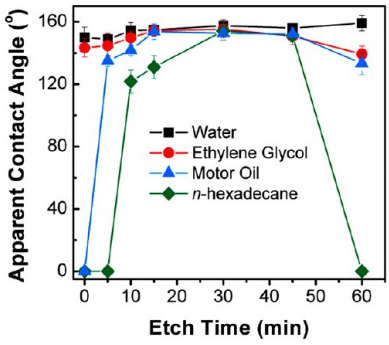

Figure 6. Contact angles of water, ethylene glycol, motor oil, and *n*-hexadecane versus etch time for 10HW handsheets made with *sec*-butanol. After 30 min of etching, handsheets demonstrate superhydrophobic and superoleophobic properties for all fluids.

deposition of a fluoropolymer layer is sufficient to render the *sec*-butanol-formed handsheets superhydrophobic, but the sheets readily absorb oils. After 5 min etch time followed by fluorocarbon deposition, stable contact angles can be measured for motor oil, and after 10 min etch time followed by fluorocarbon deposition, hexadecane droplets are repelled. Etching for 30 min followed by fluorocarbon deposition yields a surface that supports $\theta^{*}>150°$ for all four test fluids (θ_{water}^{*} = 157 ± 3°, ($\theta_{ethylene\ glycol}^{*}$ = 155 ± 5°), ($\theta_{motor\ oil}^{*}$ = 152 ± 4°), ($\theta_{n\text{-hexadecane}}^{*}$ = 154 ± 2°). Samples are observed to maintain high contact angles and repellency for 5 days. Figure 5c presents an SEM image of this surface and Figure 7 shows a

Figure 7. Droplets of four test fluids (water (dyed blue), ethylene glycol, motor oil and *n*-hexadecane (dyed red)) are shown resting on the same handsheet depicted in Figure 5c), exhibiting high contact angles for all fluids.

picture of all four test fluids resting on a single handsheet. Slide-off angles (ω) of 6 μL fluid droplets on the surface depicted in Figures 5c and 7 are as follows: ω_{water} = 13 ± 3°, $\omega_{ethylene\ glycol}$ = 19 ± 4°, $\omega_{motor\ oil}$ = 34 ± 6°; *n*-hexadecane droplets remain pinned on the surface even after inversion. Droplets of water, ethylene glycol, and motor oil can be removed without leaving

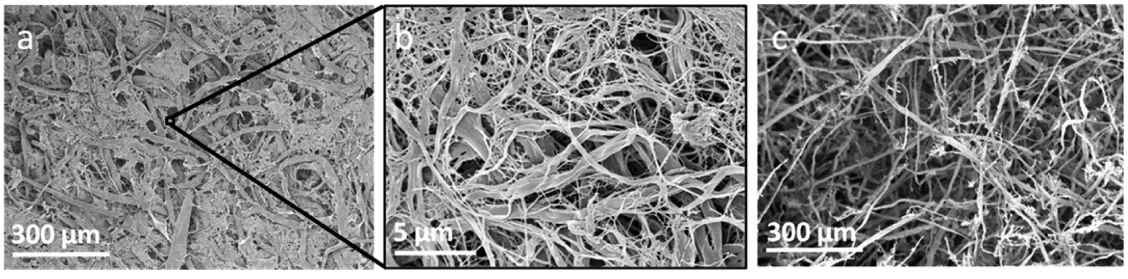

Figure 5. (a, b) Low- and high-resolution SEM images of a 10HW handsheets processed using *sec*-butanol before etching. (c) Image of the same material after 30 min of plasma etching.

dx.doi.org/10.1021/am401436m | ACS Appl. Mater. Interfaces 2013, 5, 5381–5386

residual fluid on the sheet, but a stain of *n*-hexadecane remains on the surface when the droplet is withdrawn. The staining by *n*-hexadecane is likely due to the fact that although a high apparent contact angle is observed, the droplet resides in essentially a Wenzel wetting state, leading to higher adhesion to at least some of the supporting fibers. To the best of our knowledge, this is the first report of a superamphiphobic fiber-based paper substrate that uses the inherent structure of the paper and control of the paper-making process to achieve specific wetting properties.

From SEM images, it is evident that both the solvent exchange and plasma processing steps increase the handsheet porosity. To quantify these effects, we present in Table 1

Table 1. Average Roughness (R_a) and Areal Coverage of the Top Layer of Fibers for 0, 3, and 10HW Handsheets under Different Processing Conditions (water vs. *sec*-butanol, variable etch times)[a]

handsheet type	processing fluid	etch time (min)	roughness (R_a) (μm)	areal coverage of top layer of fibers (%)
0HW	water	0	9.2 ± 0.5	77.3 ± 1.4
3HW	water	0	6.0 ± 0.6	85.2 ± 2.6
10HW	water	0	4.7 ± 1.1	99.8 ± 0.2
10HW	*sec*-butanol	0	31.7 ± 3.9	85.2 ± 0.7
10HW	*sec*-butanol	15	52.2 ± 5.4	69.5 ± 4.9
10HW	*sec*-butanol	30	53.6 ± 3.6	49.9 ± 8.7
10HW	*sec*-butanol	45	53.7 ± 3.6	54.5 ± 1.5

[a] R_a values reflect the height difference between the surface layer and underlying fiber layers; areal coverage values represent the surface porosity of the handsheets.

profilometer measurements of 0, 3 and 10HW handsheets prepared with water and *sec*-butanol that have been used to establish the average roughness (R_a) and the areal coverage of the top layer of fibers. R_a is presented in lieu of fiber surface area since it is a measure of the surface properties of the paper substrate, whereas fiber surface area measures bulk properties, which may not always be representative of the topmost layer of the paper that dominates liquid-fiber contact. A dramatic increase in R_a is observed between 10HW handsheets drained with water and *sec*-butanol. This increase in R_a is critical to maintain the Cassie–Baxter wetting state, because low roughness enables the fluid to contact fibers below the surface layer, thereby causing a transition to the Wenzel state. The surface porosity is indicated by measurements of the surface coverage, where lower values correspond to a more porous surface structure. Initially, the water and *sec*-butanol 10HW handsheets exhibit relatively similar coverage values. It is only after etching that the coverage is reduced, creating the necessary porosity to support low surface tension fluids in the Cassie–Baxter state. Although eq 1 proved very useful in this research as a guide to establish the necessary fiber size and spacings needed for superoleophobicity, a quantitative comparison with our measurements is not straightforward and is beyond the scope of the work presented here. Determining the fiber spacings in a three-dimensional network of randomly oriented fibers with a broad size distribution and noncylindrical shapes (see inset in Figure 1a) is a nontrivial task. SEM images and profilometer data presented above provide some insight, but do not characterize the three-dimensional geometry in sufficient detail to enable modeling. Furthermore, it is unclear how to interpret this information, in light of the fact that wetting models have to date only been developed for structured substrates with well-defined length scales;[45,46] for example, the average fiber spacing and size may have little physical meaning with regards to quantitative predictions of wetting properties, which are likely dominated by the extremes of the size and spacing distribution rather than their means. Nevertheless, we can conclude that eq 1 is useful for the development of less-structured fibrous substrates with great practical relevance for a variety of wetting scenarios.

CONCLUSION

In summary, we have developed a novel method to design and create paper or cellulose-based natural materials that are superamphiphobic: simultaneously superhydrophobic and superoleophobic. Pulp refining creates the appropriate diameter fibers that help stabilize the Cassie–Baxter wetting state. However, when handsheets are fabricated by draining and drying from an aqueous pulp, strong fiber–fiber hydrogen bonding causes fibers to agglomerate, reducing the overall porosity. By forming handsheets using a mixture of *sec*-butanol and water, interfiber bonding is inhibited, allowing fiber separation. Finally, by etching the handsheets with an oxygen plasma, and then performing a plasma-assisted fluoropolymer deposition, superoleophobic properties are achieved. Handsheets processed in this manner exhibit contact angles greater than 150° for water, ethylene glycol, motor oil and *n*-hexadecane. While the solvent processing assists in creating the necessary surface structures for superamphiphobicity, it also adversely affects the handsheet strength. Further studies are underway to enhance the paper strength through alteration of the solvent exchange sequence and/or subsequent processing of the handsheet. Development of superamphiphobic paper surfaces will facilitate novel applications where water and oil absorption must be inhibited simultaneously. Furthermore, the techniques, design parameters, and physical insight established in this study are applicable to other fibrous materials with randomized structures, such as nonwovens. That is, the results described in this paper permit control of wetting characteristics for virtually any fiber-based substrate by altering the fiber size and spacing during and after substrate fabrication.

AUTHOR INFORMATION

Corresponding Author

*E-mail: dennis.hess@chbe.gatech.edu.

Notes

The authors declare no competing financial interest.

ACKNOWLEDGMENTS

The authors thank the Institute of Paper and Technology (IPST) at the Georgia Institute of Technology for funding support of L. Li. The authors also thank Dr. Ashwini Sinha (Praxair) for generously donating the pentafluoroethane gas.

REFERENCES

(1) Quere, D. *Ann. Rev. Mater. Res.* **2008**, *38*, 71–99.
(2) Roach, P.; Shirtcliffe, N. J.; Newton, M. I. *Soft Matter* **2008**, *4*, 224–240.
(3) Gao, L.; McCarthy, T. J. *Langmuir* **2006**, *22*, 6234–6237.
(4) Marmur, A. *Langmuir* **2004**, *20*, 3517–3519.
(5) Chen, W.; Fadeev, A. Y.; Hsieh, M. C.; Oner, D.; Youngblood, J.; McCarthy, T. J. *Langmuir* **1999**, *15*, 3395–3399.
(6) Li, X. M.; Reinhoudt, D.; Crego-Calama, M. *Chem. Soc. Rev.* **2007**, *36*, 1350–1368.

(7) Ganesh, V. A.; Raut, H. K.; Nair, A. S.; Ramakrishna, S. *J. Mater. Chem.* **2011**, *21*, 16304−16322.
(8) Tuteja, A.; Choi, W.; Ma, M. L.; Mabry, J. M.; Mazzella, S. A.; Rutledge, G. C.; McKinley, G. H.; Cohen, R. E. *Science* **2007**, *318*, 1618−1622.
(9) Liu, Y.; Xiu, Y. H.; Hess, D. W.; Wong, C. P. *Langmuir* **2010**, *26*, 8908−8913.
(10) Shibuichi, S.; Yamamoto, T.; Onda, T.; Tsujii, K. *J. Colloid Interface Sci.* **1998**, *208*, 287−294.
(11) Xi, J. M.; Feng, L.; Jiang, L. *Appl. Phys. Lett.* **2008**, *92*, 053102.
(12) Kumar, R. T. R.; Mogensen, K. B.; Boggild, P. *J. Phys. Chem. C* **2010**, *114*, 2936−2940.
(13) Ahuja, A.; Taylor, J. A.; Lifton, V.; Sidorenko, A. A.; Salamon, T. R.; Lobaton, E. J.; Kolodner, P.; Krupenkin, T. N. *Langmuir* **2008**, *24*, 9−14.
(14) Im, M.; Im, H.; Lee, J. H.; Yoon, J. B.; Choi, Y. K. *Soft Matter* **2010**, *6*, 1401−1404.
(15) Martinez, A. W.; Phillips, S. T.; Whitesides, G. M. *Proc. Natl. Acad. Sci. U.S.A.* **2008**, *105*, 19606−19611.
(16) Lu, Y.; Shi, W. W.; Jiang, L.; Qin, J. H.; Lin, B. C. *Electrophoresis* **2009**, *30*, 1497−1500.
(17) Balu, B.; Breedveld, V.; Hess, D. W. *Langmuir* **2008**, *24*, 4785−4790.
(18) Balu, B.; Kim, J. S.; Breedveld, V.; Hess, D. W. *J. Adhes, Sci. Technol.* **2009**, *23*, 361−380.
(19) Yang, H.; Deng, Y. *J. Colloid Interface Sci.* **2008**, *325*, 588−593.
(20) Li, S. H.; Zhang, S. B.; Wang, X. H. *Langmuir* **2008**, *24*, 5585−5590.
(21) Jin, H.; Kettunen, M.; Laiho, A.; Pynnonen, H.; Paltakari, J.; Marmur, A.; Ikkala, O.; Ras, R. H. A. *Langmuir* **2011**, *27*, 1930−1934.
(22) Aulin, C.; Netrval, J.; Wagberg, L.; Lindstrom, T. *Soft Matter* **2010**, *6*, 3298−3305.
(23) Aulin, C.; Yun, S. H.; Wagberg, L.; Lindstrom, T. *ACS Appl. Mater. Inter.* **2009**, *1*, 2443−2452.
(24) Wang, X. L.; Hu, H. Y.; Ye, Q.; Gao, T. T.; Zhou, F.; Xue, Q. J. *J. Mater. Chem.* **2012**, *22*, 9624−9631.
(25) Jin, C. F.; Jiang, Y. F.; Niu, T.; Huang, J. G. *J. Mater. Chem.* **2012**, *22*, 12562−12567.
(26) Lee, H. J.; Willis, C. R.; Stone, C. A. *J. Mater. Sci.* **2011**, *46*, 3907−3913.
(27) Darmanin, T.; Guittard, F. *J. Mater. Chem.* **2009**, *19*, 7130−7136.
(28) Liu, M.; Wang, S.; Wei, Z.; Song, Y.; Jiang, L. *Adv. Mater.* **2009**, *21*, 665−669.
(29) Steele, A.; Bayer, I.; Loth, E. *Nano Lett.* **2009**, *9*, 501−505.
(30) Yang, J.; Zhang, Z. Z.; Men, X. H.; Xu, X. H.; Zhu, X. T. *New J. Chem.* **2011**, *35*, 576−580.
(31) Choi, W.; Tuteja, A.; Chhatre, S.; Mabry, J. M.; Cohen, R. E.; McKinley, G. H. *Adv. Mater.* **2009**, *21*, 2190−2195.
(32) Chhatre, S. S.; Tuteja, A.; Choi, W.; Revaux, A.; Smith, D.; Mabry, J. M.; McKinley, G. H.; Cohen, R. E. *Langmuir* **2009**, *25*, 13625−13632.
(33) Leng, B.; Shao, Z.; de With, G.; Ming, W. *Langmuir* **2009**, *25*, 2456−2460.
(34) Kota, A. K.; Li, Y. X.; Mabry, J. M.; Tuteja, A. *Adv. Mater.* **2012**, *24*, 5838−5843.
(35) Hoefnagels, H. F.; Wu, D.; de With, G.; Ming, W. *Langmuir* **2007**, *23*, 13158−13163.
(36) Wenzel, R. N. *Ind. Eng. Chem.* **1936**, *28*, 988−994.
(37) Cassie, A. B. D.; Baxter, S. *Trans. Faraday Soc.* **1944**, *40*, 0546−0550.
(38) Michielsen, S.; Lee, H. J. *Langmuir* **2007**, *23*, 6004−6010.
(39) Marmur, A. *Langmuir* **2003**, *19*, 8343−8348.
(40) *Laboratory Beating of Pulp (PFI mill method) Test Method T 248 sp-08*; Technical Association of the Pulp and Paper Industry: Peachtree Corners, GA, 2008.
(41) Ek, M.; Gellerstedt, G.; Henriksson, G. *Pulp and Paper Chemistry and Technology: Paper Products Physics and Technology*; Walter de Gruyter & Co: Berlin, Germany, 2009; Vol. 4.
(42) Steenkamer, D. A.; McKnight, S. H.; Wilkins, D. J.; Karbhari, V. M. *J. Mater. Sci.* **1995**, *30*, 3207−3215.
(43) Haselton, W. R. An investigation of the adsorption of gases by wood and its componenets and of gas adsorption techniques as a means of studying the area and structure of pulp and paper. *Ph.D. Thesis*, Lawrence College, Appleton, WI, 1953.
(44) Robertson, A. A. *Tappi* **1970**, *53*, 1331−1339.
(45) Tuteja, A.; Choi, W.; Mabry, J. M.; McKinley, G. H.; Cohen, R. E. *Proc. Natl. Acad. Sci. U.S.A.* **2008**, *105*, 18200−18205.
(46) Blow, M. L.; Yeomans, J. M. *Langmuir* **2010**, *26*, 16071−16083.